Hydrometeorological Reconstructions for Northeastern Mongolia Derived from Tree Rings: AD 1651-1995

Neil Pederson[1], Gordon C. Jacoby[1], Rosanne D. D'Arrigo[1], Edward R. Cook[1], Brendan M. Buckley[1], Chultemiin Dugarjav[2], and R. Mijiddorj[3]

[1]Tree-Ring Laboratory, Lamont-Doherty Earth Observatory*, Palisades, NY
[2]Institute of Biotechnology, Ulaanbaatar, Mongolia
[3]Hydrometeorological Research Institute, Ulaanbaatar, Mongolia

Abstract

Reconstructions of annual (prior August-current July) precipitation and streamflow, 345 years in length (AD 1651-1995), are presented for northeastern Mongolia based on tree-ring width data. These precipitation and streamflow reconstructions account for 54% and 48% of the respective variance in instrumental data over the past 50 years. Variations in instrumental precipitation and streamflow are within the range of those reconstructed over the length of tree-ring record. However, there appear to be more frequent extended wet periods during the 20th century. Multitaper spectral analysis revealed statistically significant peaks at 10.8 and 12.8 years for the precipitation reconstruction, and at 12.8 and 20.3-23.8 years for the streamflow reconstruction. Similarly, singular spectrum analysis identified spectral modes of variation at 12 and 21 years for both series. These spectra resemble those found for tree-ring based precipitation reconstructions in central China as well as the western USA, and may reflect solar influences on the climate of Mongolia.

1. Introduction

Fluctuations in precipitation profoundly impact the agrarian economy and nomadic segment of Mongolian culture. In 1999 a severe summer drought followed by heavy winter snowfall triggered starvation and death of an estimated two million of the nation's livestock. Mongolia is characterized by an extremely continental climate, predominantly influenced by the Siberian High pressure cell, also called the Mongolian or Asiatic High, which is often centered over northern Mongolia from winter through late spring (Zhang and Lin 1992; An and Thompson 1998; Samel et al. 1999). Mongolia is situated where the mid-westerly jet converges with monsoonal airflow from the southwest (Yatagai and Yasunari 1995). Other circulation systems that influence central Asia precipitation are the east Asia Monsoon (Xue 1996; An and Thompson 1998; Samel at al. 1999), Indian Summer-Monsoon (Yatagai and Yasunari 1995; Xue 1996), north Pacific High (Yatagai and Yasunari 1995), and El Niño /Southern Oscillation (Yatagai and Yasunari 1994; Mijiddorj and Jigmeddorj 1995; Yatagai and Yasunari 1995; Meiyu et al. 1995). Mongolia lies near the limit of these effects and apparently no single system consistently dominates the climate. In summer, local radiation balances and convective storms influence Mongolian climate (Zhang and Lin 1992).

A study of instrumental precipitation data for eastern Mongolia indicates that summer rainfall has increased since the 1940s (Dagvadorj and Mijiddorj 1996), while a concomitant decrease since the 1950s has been observed in southern Mongolia (Yatagai and Yasunari 1995). A recent study of dry and wet intervals around the globe from 1900-1995 found a slight increase in extreme events and areal coverage of severe drought or moisture surplus in some areas of Asia since the late 1970s (Dai and Trenberth 1998). General circulation model experiments suggest that drought variations at middle to high northern latitudes (such as Mongolia) may become more frequent or extreme under conditions of elevated temperature (e.g. Kattenburg et al. 1996). Such analyses illustrate the need for longer records in order to place these recent or projected changes into long-term perspective for Mongolia and elsewhere in northern Asia.

Tree rings have been employed successfully to reconstruct precipitation, streamflow (which integrates precipitation over an entire drainage basin), and other meteorological variables for many areas of the Earth (e.g. Schulman 1945; Stockton and Jacoby 1976; Cook and Jacoby 1983; Cleaveland and Stahle 1989; D'Arrigo and Jacoby 1991; Boninsegna 1992; Grissino-Mayer 1996; Cook et al. 1997). Yet few such reconstructions exist for northern and central Asia, and these are mainly in China (Wu 1992; Hughes et al. 1994) with almost no such records available for Mongolia. A recent study presented a temperature-

sensitive tree-ring record of Siberian pine from alpine treeline (2290 m) in the Tarvagatay Mountains of north central Mongolia (Jacoby et al. 1996). In this paper, we present some of the first hydrometeorological reconstructions for this region, based on drought-sensitive trees from lower-forest border sites in northeastern Mongolia. These reconstructions provide a long-term perspective for drought variations recorded in the instrumental data over the past fifty years. They also yield longer time series with which to begin to consider the relative roles of natural climate forcings versus possible anthropogenic influences on precipitation over the past several centuries.

2. Data and Methods:
a. Tree-Ring Records

Standard dendrochronological techniques were applied in this analysis (Stokes and Smiley 1968; Fritts 1976; Holmes 1983; Cook and Kairiukstis 1990). Trees at or near the forest-grassland ecotone (i.e. lower forest border) are often moisture stressed and record varying precipitation in their annual ring widths (Fritts 1976). Since our interest for this study was the reconstruction of hydrometeorological variables, we selected trees from lower forest border sites where there was little or no apparent evidence of human or other disturbance. These sites were characterized by having widely spaced trees and sparse ground vegetation, both indicators of a drought-stress environment.

Two such sites were found in northeastern Mongolia. One of these was a Scots pine (*Pinus sylvestris* L.) lower forest border site at Urgun Nars (UN), at 48° 34.6′N, 110° 32.7′E, elevation 1070 m (Figure 1). The other location sampled was for Siberian larch (*Larix sibirica* Ledebour) from a disjunct stand within a semi-arid grassland ecosystem at Zuun Mod (ZM) at 47°47.2′N, 107°30.0′E, elevation 1415 m (Figure 1). In the Mongolian region, these two species are often the dominant trees in the dry lower elevation transitional vegetation zones (Price and Simpson 1913; Wang 1961).

The raw ring width measurements for these two sites were standardized using the ARSTAN method, which creates a mean-value series of ring-width indices for all samples available for each year (Cook 1985). The standardization process involved detrending of individual tree-ring series using either negative exponential, linear regression of negative slope to zero slope, or 400-year smoothing spline curve fits. With the option we selected, the ARSTAN program makes data-based decisions on whether the negative exponential detrending or linear regression is appropriate. We also selected a 400-year spline in a few cases when there appeared to be anomalous low-frequency trends different from the common trends of the rest of the trees. Our intent with this
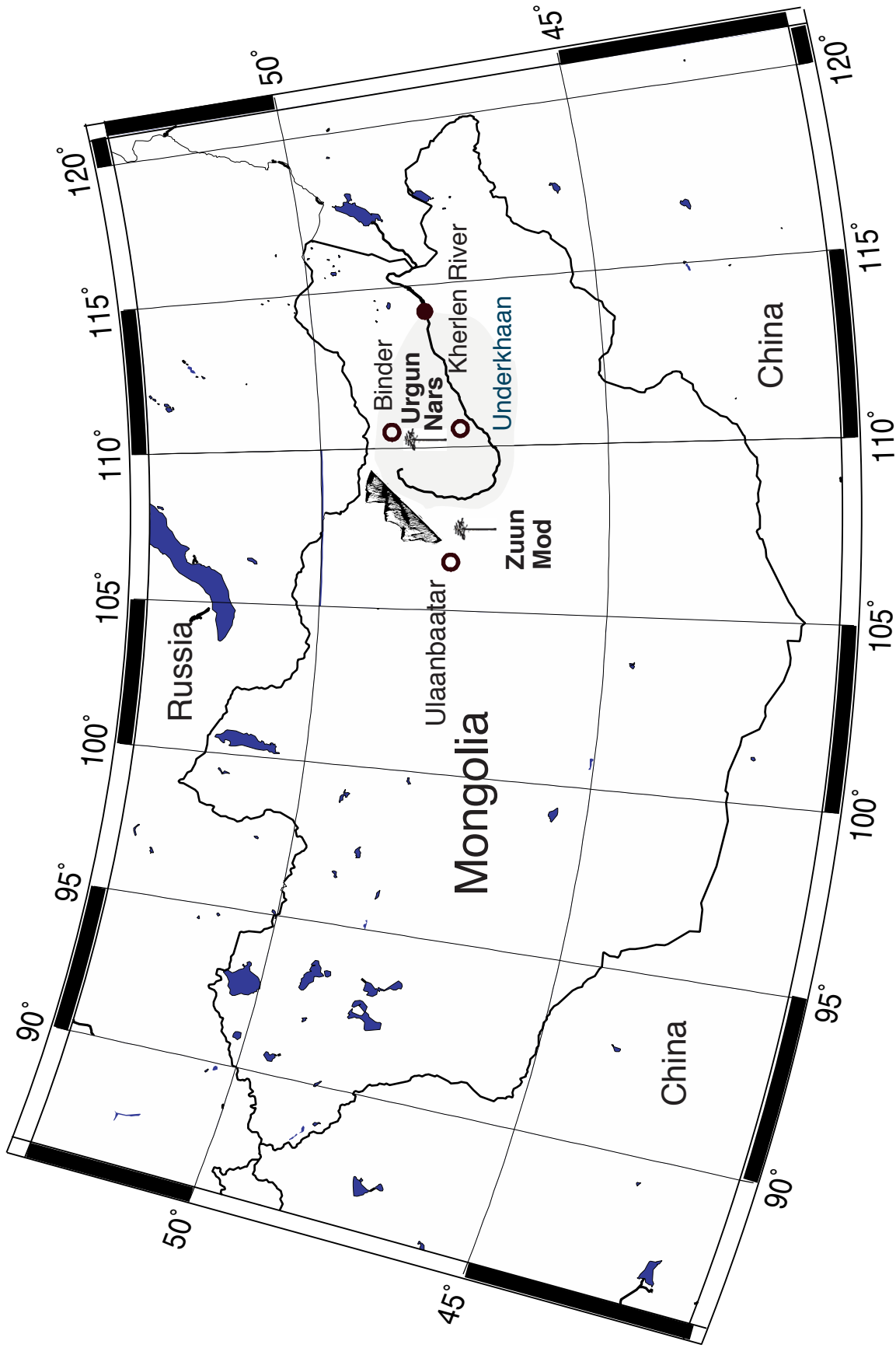
Figure 1. Location of sampling sites and meteorological stations in Mongolia. A tree symbol (🌲) represents the Urgun Nars and Zuun Mod sites. Tree site names are bold. Hollow circles (⭘) are meteorological stations. The solid circle (●) represents the streamflow gauge location. The shaded area approximates the watershed modelled. Only the mountain range of the watershed is pictured.

methodology is to remove biological growth trends while preserving variations of all frequencies that may be related to climate (Cook and Kairiustis 1990). The final UN chronology extends from AD 1651-1996, is comprised of data from 16 trees and 33 cores (with 4 series extending back to 1661 and 8 to 1668), and has a mean segment length of 189 years. The final ZM chronology dates from 1582-1996, consists of data from 13 trees and 30 individual series (with 3 cores dating back to 1583 and 10 back to 1593), and has a mean segment length of 332 years.

The Rbar (Briffa 1995) and Expressed Population Signal (EPS; Wigley 1984) statistics are two parameters for evaluating the quality of tree-ring chronologies (Cook and Kairiukstis 1990). The Rbar, the mean correlation coefficient between all tree-ring series used in a chronology, was 0.652 for UN and 0.690 for ZM. The EPS, a function of both Rbar and sample size, exceeds 0.965 for every 30-year segment over the lengths of record for both chronologies, well above the 0.85 threshold value which is considered acceptable by some researchers (Wigley 1984; Cook and Kairiukstis 1990). Based on these evaluations we consider these chronologies to be valid for use in dendroclimatic reconstruction as outlined below. Correlation functions between the tree chronologies and monthly instrumental data were calculated to identify the season for reconstruction (Figure 2).

We used the multitaper method (MTM) to evaluate the spectral properties of the reconstructions. MTM has several advantages over single taper methods, including reduced bias from data leakage, production of direct spectral estimates with multiple degrees of freedom, and a better tradeoff between spectral resolution and statistical variance than single taper methods (Percival and Walden 1993; Mann and Lees 1996). Significance tests were calculated following Mann and Lees (1996). The calculation of the null hypothesis was performed by the robust noise background estimation procedure. This method uses median smoothing of the spectrum to estimate background noise insensitive to the peaks (Mann and Lees 1996). Blackman-Tukey (BT) cross-spectral analysis (Jenkins and Watts 1968) was used to explore spectral coherency between the reconstructions and instrumental hydrometeorological records. Singular spectrum analysis (SSA) was also employed to further explore the spectral properties of the reconstructions. SSA is a data-adaptive method for extracting oscillatory signals from noise in time series (Vautard 1995). Maximum entropy spectral analysis (MEM) was used to explore the spectral properties of the bidecadal waveforms extracted by SSA (Marple 1987). The autoregressive component used in MEM analysis was the prediction error filter length, which is 20% of the series length. Using multiple spectral analysis methods helped to evaluate the stability of the spectral properties.
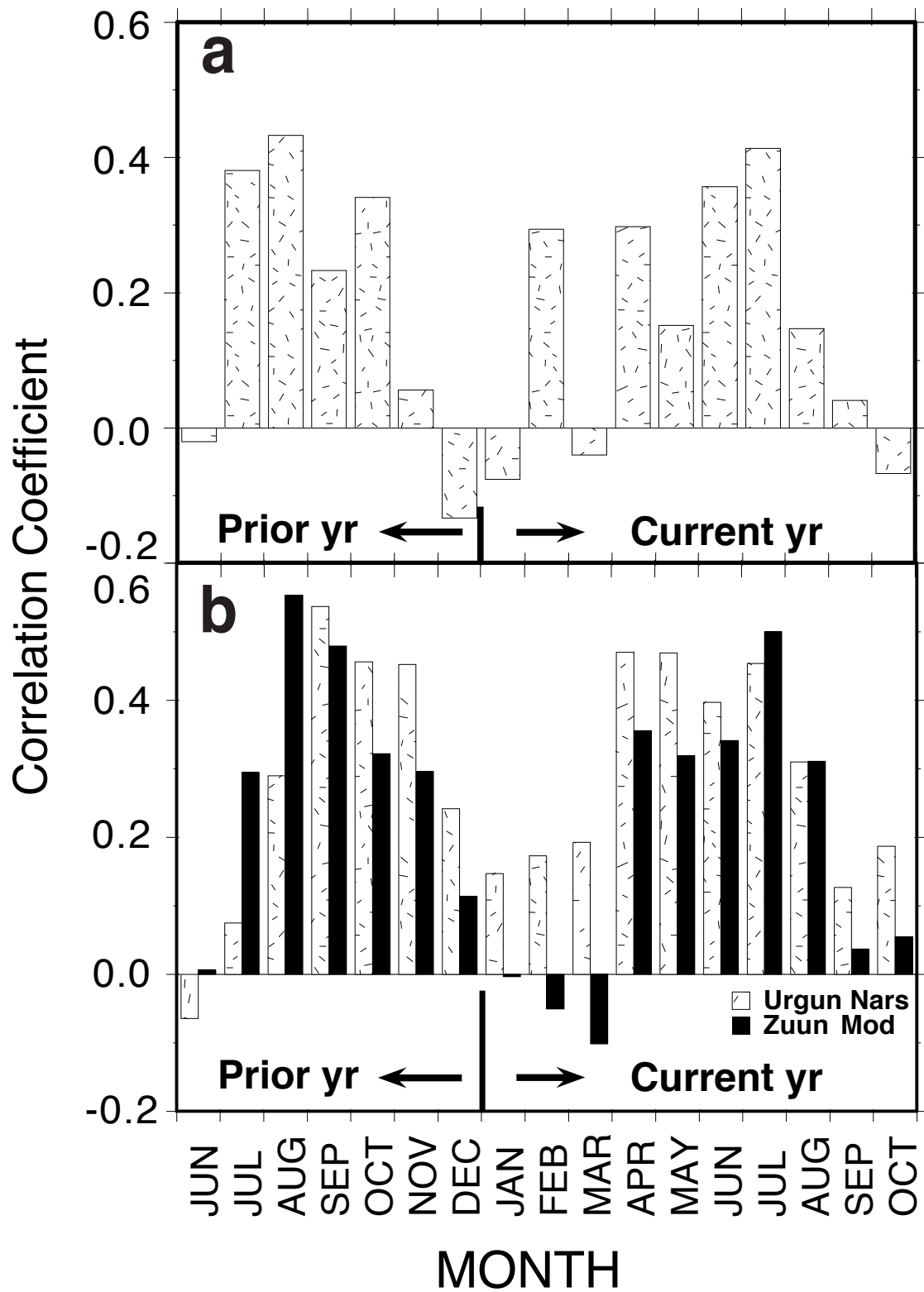
Figure 2. Monthly correlation coefficients of a) Urgun Nars tree-ring chronology and instrumental precipitation data and b) Urgun Nars (stipled bars) and Zuun Mod (solid bars) tree-ring chronologies with instrumental Kherlen River streamflow data.

b. Hydrometeorological Records

1) Precipitation

Instrumental hydrometeorological records were provided by the Hydrometeorological Research Institute in Ulaanbaatar. Limiting factors of climatic reconstruction in Mongolia are short instrumental records and a low density meteorological station network. The records used for these reconstructions are the best climatic time series available for the region of this study. For dendroclimatic modeling, hydrometeorological data must have sufficient length for regression analysis.

Precipitation records used were the only three long and continuous meteorological stations close to the tree-ring sites: Binder, Ulaanbaatar, and Underkhaan (Figure 1). All station records were significantly correlated with each other (r ranging 0.36-0.56; p-value <0.05) over the dendroclimatic year modeled indicating spatial coherency. These series were averaged over the common interval from 1941-1995. Averaging precipitation records from different stations can decrease small-scale noise and improve statistical relationships between trees and meteorological data (Blasing et al. 1981). Mean annual precipitation for this three-station average is 278.6 mm (standard deviation (SD) 56.3 mm), with summer (June-August) rainfall accounting for nearly 74% of the total.

2) Streamflow

Monthly streamflow data for the Kherlen River at the Choibalsan hydrologic station (Figure 1) were available from 1947-1994. There are no significant reservoirs or diversions of the Kherlen River above the gauge point. Mean annual streamflow is 253.14 m^3 per second (SD 116.85). Data from two of the precipitation stations are located within this drainage basin; hence the meteorological series are not independent from the streamflow data.

3. Results

a. Hydrometeorological reconstructions

1) Precipitation

The best precipitation model, obtained using linear regression techniques (Cook and Kairiukstis 1990), was derived using the UN tree-ring record alone;

6

addition of the ZM chronology did not improve the results. ZM correlated more highly with the streamflow data (see below). The best precipitation relationship was found when the UN series was correlated with the three-station precipitation average over the months from previous August to July of the current year of growth for 1942-1995 (r = 0.742; Figure 2a,). Based on our own sampling in Mongolia in August, we observe that radial growth is nearly complete by the beginning of August. Current August precipitation has a much lower correlation with ring width than prior August (Figure 2a). Trees can respond to favorable soil moisture and photosynthetic conditions prior to the growing season, with these conditions integrated into the current year's growth ring (Fritts 1976; Kramer and Kozlowski 1979). Tree growth had a weak negative correlation to temperature during the growing season. We interpreted this as being due to the relationship of high temperature with drier conditions. Intercorrelation of the three-station precipitation and temperature instrumental data verified that temperature and precipitation are negatively correlated in northeastern Mongolia. The resulting Urgun Nars precipitation reconstruction (UNP) accounts for 54.2% of the variance (ar^2, adjusted for degrees of freedom) over the 1942-1995 calibration period (Figure 3a, Table 1). The final UNP reconstruction from AD 1651-1995 is presented in Figure 4a.

2) Streamflow

Using principal components analysis, UN and ZM series were used to predict streamflow at Kherlen River. Combining UN and ZM results in a loss of data from 1582-1650 (due to the 1651 beginning of the UN chronology). The UN and ZM chronologies responded similarly to the same season of climate (Figure 2b). There were different growth responses during the winter. Kherlen River streamflow is at an annual low from January through March (mean seasonal flow 14.1 m^3 per second [SD 29.0]) representing 5.6% of the mean annual flow. Measurements at such low flow are less reliable than higher flows (Linsley et al. 1949). Thus, the response differences at low flow and low correlation are likely unimportant. From 1948-1994, the combined UN and ZM predictors correlated at r = 0.703 for the same August-July interval used for precipitation. The Kherlen River streamflow reconstruction (KRS) model accounted for 48.2% of the variance (ar^2) over the period of calibration (Figure 3b, Table 1). The final KRS reconstruction is shown in Figure 4b.

3) Model Verification

Split-sampling calibration and verification tests were used to evaluate the quality and stability of both reconstruction models (Fritts 1976; Cook and Kairiukstis 1990). Residual analysis indicated a statistical autocorrelation in
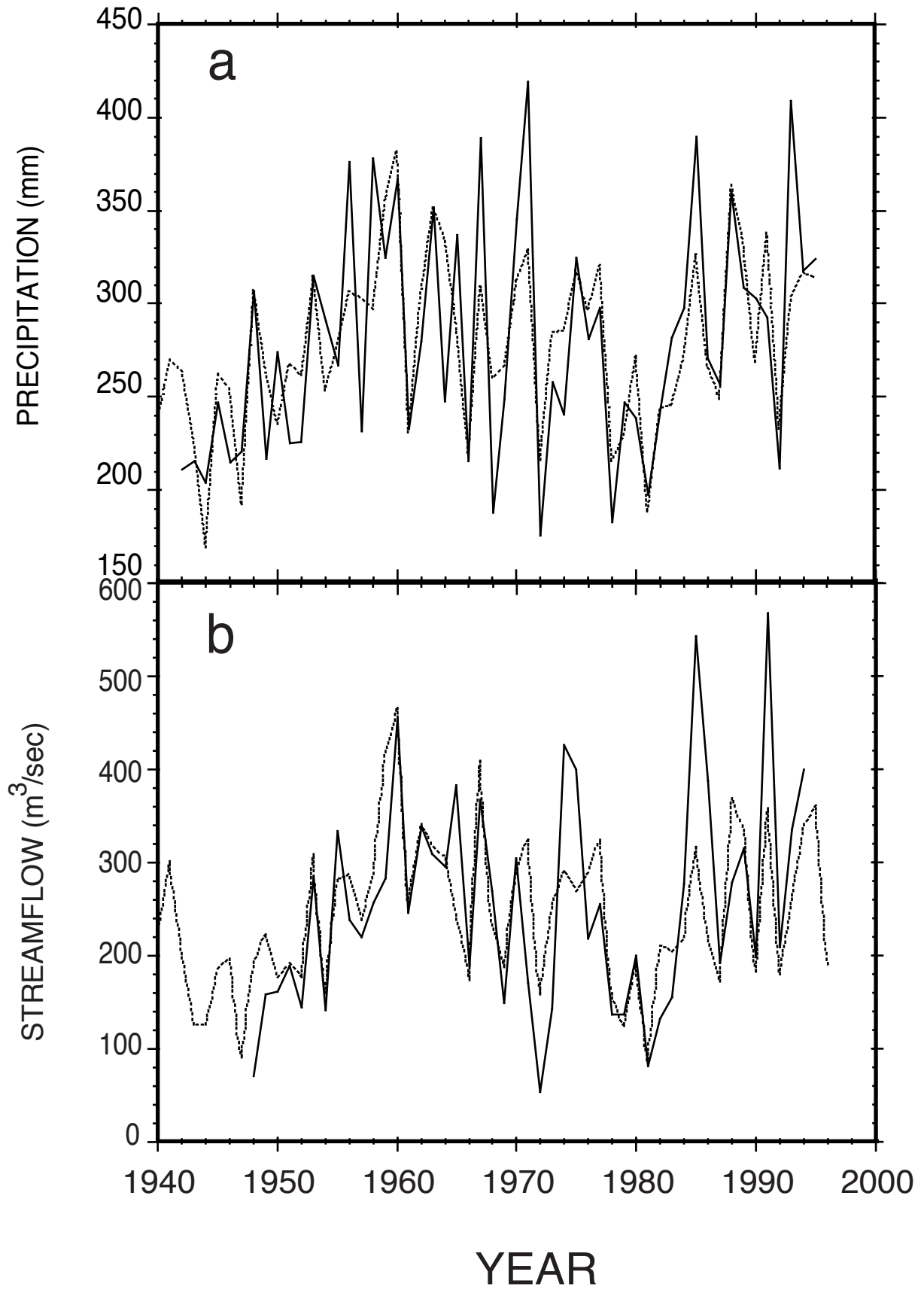
Figure 3. Recorded (solid line) and reconstructed (dashed line) a) Urgun Nars precipitation from 1942-1995 and b) Kherlen River streamflow from 1948-1994.

Table 1. Reconstruction statistics for Urgun Nars precipitation and Kherlen River streamflow dendroclimatic year (previous August through current July).

Urgun Nars

	1942-1968 Calibration	1969-1995 Verification	1969-1995 Calibration	1942-1968 Verification	1942-1995 Final Calibration
variance explained	0.475	-	0.646	-	0.550
adjusted r^2	0.454	-	0.632	-	0.542
Pearson Corr. Coef.	0.689	0.804	0.804	0.689	0.742
Reduction of Error	0.475	0.600	0.646	0.432	-
Coef. of Efficiency	0.475	0.581	0.646	0.403	-
Product Means Test	0.178(*@)	0.194(@)	0.295(@)	0.229(**)	-
Sign Test	22+/5-(*@)	24+/3-(@)	22+/5-(*@)	22+/5-(*@)	-

Kherlen River

	1948-1970	1971-1994	1971-1994	1948-1970	1948-1994
variance explained	0.649	-	0.450	-	0.494
adjusted r^2	0.632	-	0.425	-	0.482
Pearson Corr. Coef	0.805	0.681	0.670	0.825	0.703
Reduction of Error	0.649	0.395	0.450	0.442	-
Coef. of Efficiency	0.649	0.393	0.450	0.438	-
Product Means Test	5090.6(**)	8202.2(@)	9090.9(**)	7832.0(**)	-
Sign Test	20+/3-(@)	17+/7-(*)	18+/6-(*)	21+/2-(@)	-

Common period is meteorological data tested is 1942-1995 for Urgun Nars and 1948-1994 for Kherlen River. adjusted r^2 = variance explained adjusted for loss of degrees of freedom; (*) = level of probability <0.05; (**) = level of probability <0.01; (*@) = level of probability <0.002; (@) = level of probability <0.001.
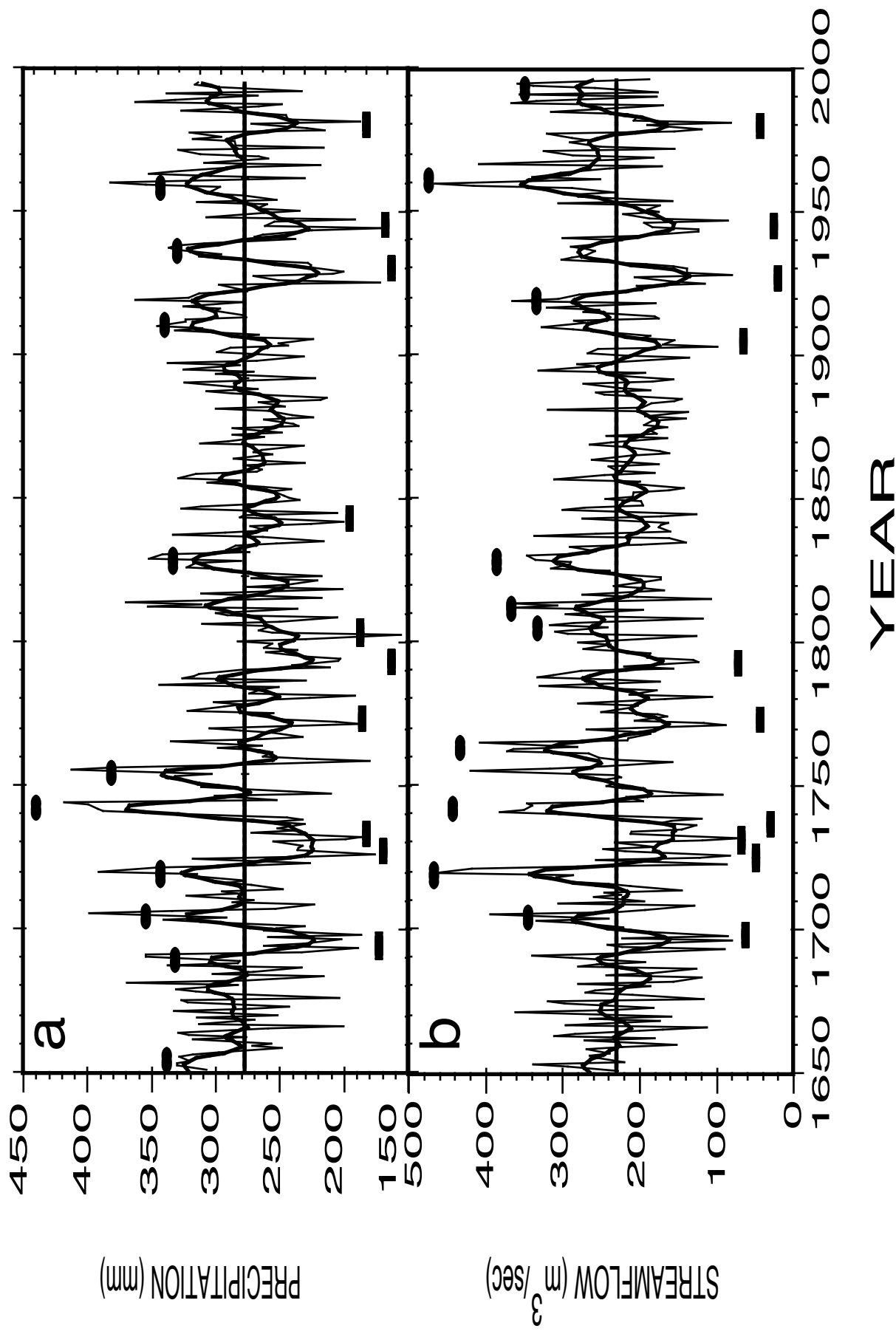
Figure 4. Reconstruction of a) Urgun Nars precipitation and b) Kherlen River streamflow. The thin line is reconstructed data. The thick, curvilinear line is the 10 year cubic smoothing spline. The solid, flat line is the reconstruction mean. Filled ovals signify extreme wet intervals. Filled rectangles signify extreme dry intervals. Extreme intervals were averaged over 5 year periods and ranked to identify the top 10 wet and dry five-year intervals.

the streamflow reconstruction over the 1948-1994 period (calculated Durbin-Watson Statistic (D-W) = 1.26 for n=47; 5% significance value = 1.49. A calculated value less than the significance value indicates a significant relationship [Draper and Smith 1981]). This relationship was not significant for the 1948-1970 period, but was significant for the 1971-1994 period (calculated D-W = 1.08 for n = 24; significance D-W = 1.27). Inspection of the instrumental streamflow data indicated that 3 unusual years (1985, 1986, 1991) account for much of the trend. Removing these data points greatly reduced the trend in the data. A pre-whitening experiment gave the following results: 1) the trend in the instrumental data was not significant and 2) pre-whitening of the tree-ring data did not produce a significantly different relationship between tree growth and streamflow. Seven verification tests were significant at the 0.001 level or better. Only sign tests for the 1971-1994 period were not significant at the 0.01 level (0.033 and 0.012, respectively; see below). The consensus of the verification tests indicate a highly significant and valid model. Therefore, we decided to use the original reconstruction.

Verification tests indicate that both reconstructions captured the low and high frequency variations of the recorded data well (Figures 2a-b) despite the fact that trees tend to underestimate extreme seasons or years (Fritts 1976; Young 1994). For example, the Reduction of Error (RE) and Coefficient of Efficiency (CE) statistics, both considered to be rigorous tests of model validation, were positive, providing evidence that the reconstructions exhibit positive skill in estimating the climate information (Fritts 1976; Cook et al. 1994; Table 1). Product means tests, a measure of the sign and magnitude of departure from the calibration mean, were significant at or above the .01 level. The sign test results, an indication of how well the tree-ring estimates track the direction of change in climate from year to year, were significant at or above the .05 level for both series.

4) Evaluation of Hydrometeorological Data

The three-station precipitation data were used to estimate the streamflow data for intercomparison with the tree-ring estimates. Both trees and streamflow integrate evapotranspiration effects in addition to precipitation input. Analysis of the precipitation-streamflow data showed that the preceding month's precipitation is the best estimator for current month streamflow. Therefore, a 12-month total precipitation for July through June was used to estimate August through July streamflow (the hydrologic year estimated by the tree-ring data). Results showed that the precipitation accounted for 38.5% of the variance (ar^2) in streamflow, notably less than the

tree-ring estimates. Using only the two rain gages within the Kherlen River basin produced even poorer results. Based on the area of a standard rain gage and the total area of root extension for trees sampled at each site, tree-ring sampling covers orders of magnitude more surface area than the three rain gages. Stahle and Cleaveland (1992) found that a single met station explained only 6-13% more precipitation variation than tree-ring chronologies in the southeastern United States. Thus, tree-ring records can make good estimates of regional moisture conditions.

5) Hydrometeorological Variability

To evaluate precipitation and streamflow variability over the lengths of the reconstructions, we calculated the ten most extreme non-overlapping wet and dry five-year intervals for both reconstructions (Table 2). Compared to the rest of the reconstruction, unusual clustering of extreme wet or dry intervals was not obvious in the modern period (Figure 4a-b). Further, the standard deviation of UNP was slightly lower from 1942-1995 (46.6) than from 1651-1850 (50.2), the interval prior to a period of reduced amplitude from 1847-1907 (see below). However, for KRS, the SD was higher for 1948-1994 (82.35) relative to 1651-1850 (SD 75.65). There is some indication of extended wetter periods in the 20th century, especially the 1900s to 1920 and 1950s to 1960s (Figure 4a, b). Although it is possible that the variable periods in the early parts of these records may be related to a decreasing sample size, the strong EPS statistics suggest this is probably not the case.
One feature of interest in both reconstructions is a period of low variability from the late 1840s to early 1900s. This feature is reflected in the SD, which is only 30.0 for the precipitation reconstruction from 1847-1907, compared to a value of 49.1 for the reconstruction excluding that time interval. Similarly, the SD for the streamflow reconstruction is 48.36 for 1847-1907, and 76.98 for the rest of the reconstruction.

6) Spectral Analysis

Using MTM methods, the instrumental precipitation record and UNP reconstruction from 1942-1995 had significant (95% level) spectral coherency at 2.0, 2.8, 4.1, 6.2, 8.3, 12.5 years with broad peaks centered at 25 and 50 years. The recorded streamflow data and the KRS reconstruction from 1947-1994 had significant (95% level) spectral coherency at 2.5-2.9, 3.5, 6.2 and 16.7 years. Due to the shortness of the instrumental hydrometeorological data, the lower-frequency results should be interpreted with caution.

Table 2 - Top 10 5-year dry and wet periods for Urgun Nars and Kherlen River reconstructions.

RANK	URGUN NARS PRECIPITATION		KHERLEN RIVER STREAMFLOW	
	TIME INTERVAL (average)			
	DRY	WET	DRY	WET
1	1928-1932 (21.8)	1740-1744 (38.9)	1925-1929 (139.6)	1959-1963 (357.8)
2	1791-1795 (21.8)	1752-1756 (35.3)	1943-1947 (142.5)	1717-1721 (354.6)
3	1943-1947 (22.1)	1702-1706 (33.6)	1725-1739 (144.6)	1740-1744 (342.8)
4	1725-1729 (22.2)	1717-1721 (32.9)	1771-1775 (150.7)	1761-1765 (338.2)
5	1692-1696 (22.4)	1956-1960 (32.9)	1978-1982 (151.0)	1826-1830 (315.6)
6	1978-1982 (23.0)	1908-1912 (32.7)	1723-1727 (153.3)	1810-1814 (306.1)
7	1731-1735 (23.0)	1652-1656 (32.6)*	1696-1700 (160.4)	1991-1995 (297.9)
8	1771-1775 (23.2)	1826-1830 (32.3)	1903-1907 (161.4)	1702-1706 (296.0)
9	1801-1805 (23.3)	1687-1691 (32.2)	1729-1733 (162.6)	1917-1921 (290.3)
10	1841-1845 (23.8)	1934-1938 (32.1)	1791-1795 (164.4)	1803-1807 (289.8)

* This interval should be interpreted with caution since it is represented by only one series.

Using MTM methods over the full length of the precipitation reconstruction, UNP had significant peaks at 10.8 year (90%) and 12.8 year (95%; Figure 5a). Lower frequency peaks (not significant) were found at 16.7, 19.3 and 23.3 yr. Significant (95% level and higher) high-frequency peaks for UNP were found at 2.1, 2.7, 3.0, 3.3 and 3.5. For the full KRS reconstruction, significant peaks were identified at 12.8 and 20.3-23.8 year (95%; Figure 5b). Significant (95% level and higher) high-frequency peaks for KRS were found at 2.2-2.3, 2.7, 3.1, and 3.4-3.6. We concentrated our analyses on the low-frequency peaks to evaluate bidecadal drought.

The dominant waveforms extracted with SSA (using a 60 year lag) for UNP were at 12.3 (eigenvector pair 2 and 3) and 21.3 year (pair 5 and 6). These waveforms accounted for 9.75 and 8.06% of the total variation, respectively. Using a 100 year lag for KRS, waveforms were extracted for 12.2 (eigenvector pair 3 and 4), 18.0 (pair 7 and 8), 21.7 (pair 1 and 2), and 50 (pair 5 and 6) years. These periodicities accounted for 7.19, 4.69, 10.72 and 4.64% of the streamflow variation, respectively.

In KRS, the above noted reduction in variability from about 1850-1900 appears to coincide with an out of phase relationship between the 18.0 and 21.7 year waveforms extracted from SSA (Figure 6a, c). Conversely, greater variability is seen when these two modes are in phase (Figure 6a, c). The 21-year waveform for UNP shows similar fluctuations in time and amplitude (Figure 6b). MEM analysis of the UNP 21-year waveform shows that it is comprised of 18.2 and 21.3 year periodicities (Figure 7). In both reconstructions, changes in variability and extreme 5 year episodes (Figure 4a, b) appear to coincide temporally with changes in the phase relationship of the 18 and 22 year waveforms (Figure 6c).

The existence of bidecadal periodicity in these reconstructions suggests the possibility of solar influence (Mitchell et al. 1979; Stockton et al. 1983; Hoyt and Schatten 1997; Cook et al. 1997). Blackman-Tukey cross-spectral analysis between KRS, the reconstruction with the strongest and most consistent bidecadal waveform, and the annual Wolf sunspot numbers (obtained from the National Geophysical Data Center and characterized by a significant, broad band of spectral power at 7.6-13.1 years) for the common period 1700-1995 revealed significant (95% level) coherency at 20-23 years. The 11-year sunspot cycle has magnetic polarity in alternating cycles forming the 22-year Hale magnetic solar cycle (Hale 1924; Shove 1983) which has been hypothesized as having influence on drought cycles (Mitchell et al. 1979; Stockton et al. 1983; Cook et al. 1997).
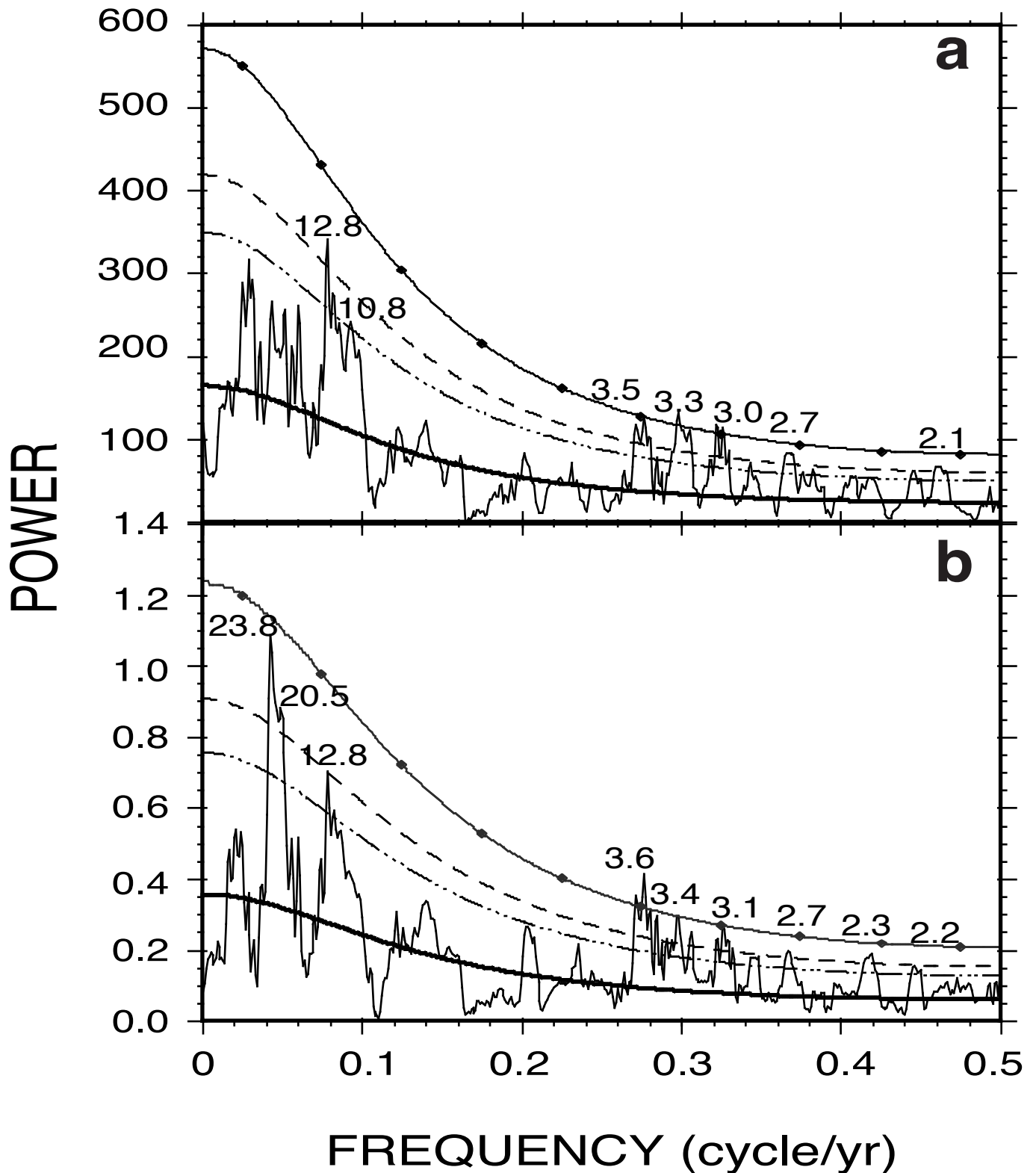
4. Discussion

Figure 5. MTM spectral densities of a) Urgun Nars precipitation reconstruction and b) Kherlen River streamflow reconstruction. The thick solid line = the null hypothesis. Dot and dashed line = the 90% confidence level; Dashed line = 95%; Solid line with diamonds = 99%. Centers of the peaks are labeled in years. The null hypothesis was determined using the robust noise background estimation procedure (Mann and Lees, 1996).
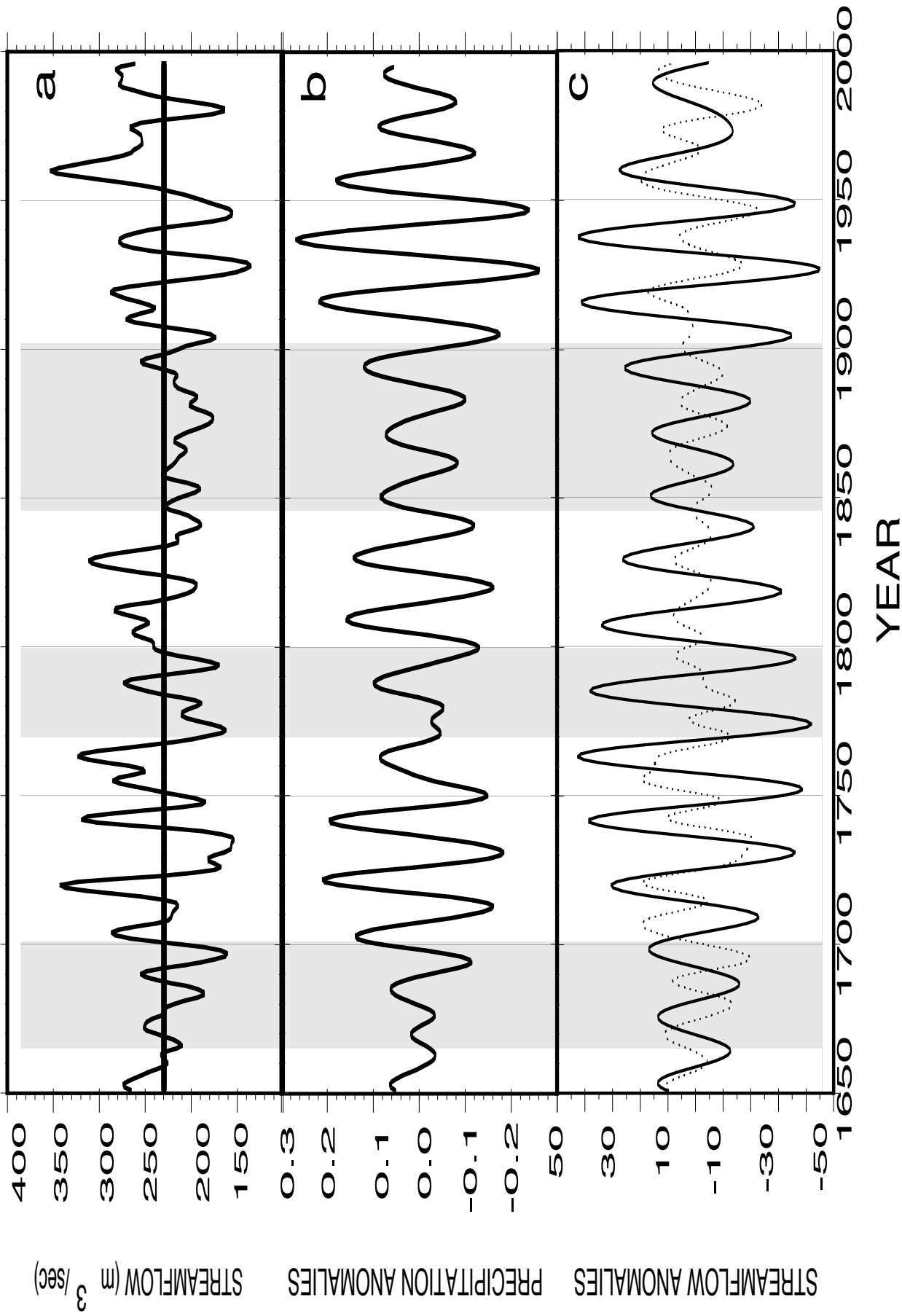
Figure 6. a) 10 year running average of the Kherlen River streamflow reconstruction (KRS-1). The solid, flat line shows the reconstruction mean. b) 21 year waveform of UNP extracted by SSA. c) The 22 (thick line) and 18 (dashed line) year waveforms extracted from KRS-1 using SSA. The shaded areas show intervals of reduced streamflow (a) and precipitation amplitude (b) that correspond to intervals when the 22 and 18 year waveforms are out of phase (c).
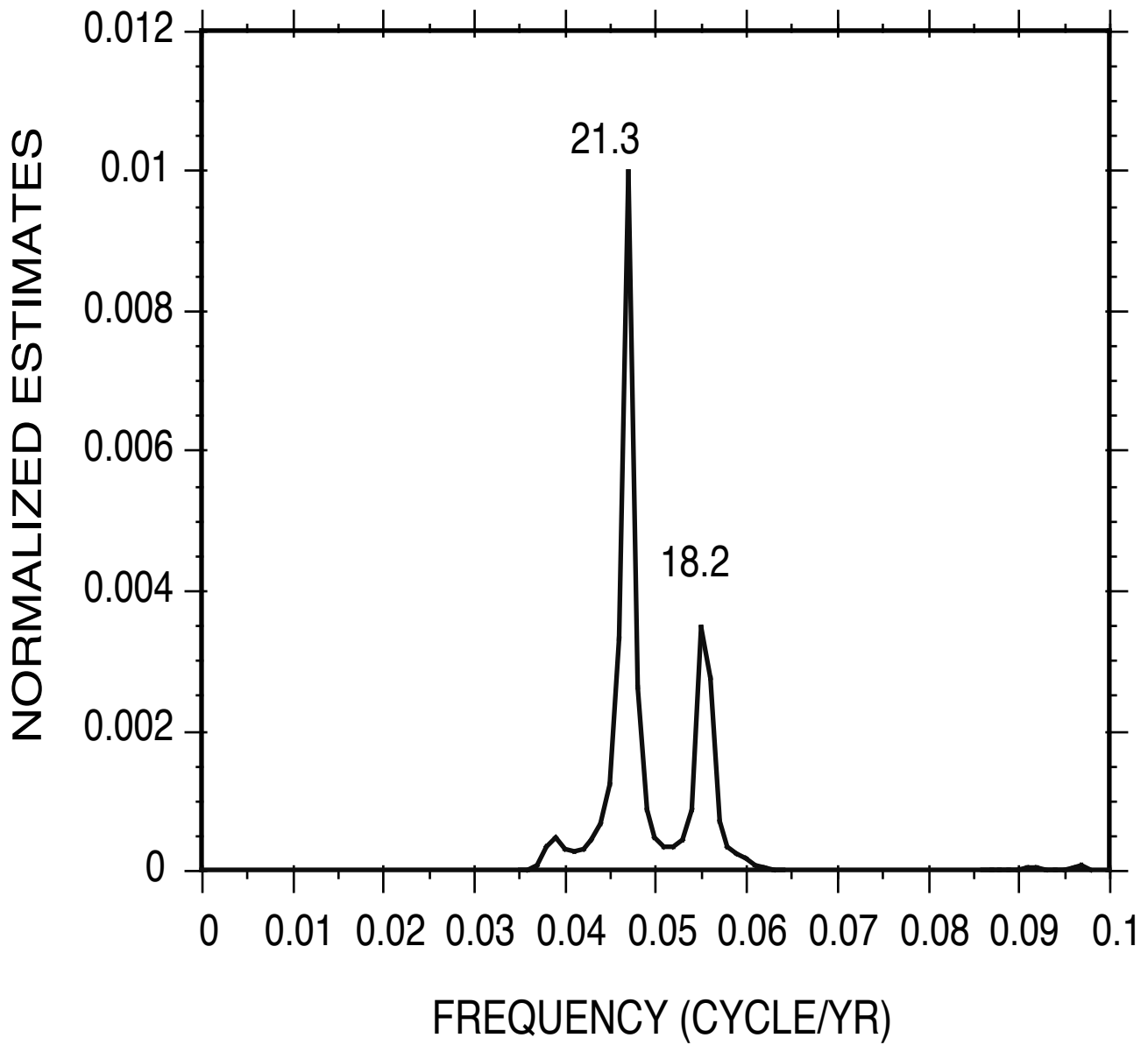
Figure 7. MEM spectrum of the UNP 21 year waveform. Centers of the peaks are labeled in years.

The reconstructions presented herein for northeastern Mongolia provide longer time series for evaluation of precipitation and streamflow variability, extending the available instrumental record by nearly 300 years. Our evaluations of both standard deviation and extreme dry and wet five-year intervals suggest that variations over the recent period of instrumental data are not unusual relative to the prior record. Previous analysis of recorded precipitation data for Mongolia indicated an increase in summer precipitation over the past half century (Dagvadorj and Mijiddorg 1996). Inspection of the UNP and KRS reconstructions shows several periods of decadal oscillations (Figure 4a, b), suggesting that the trend from 1942-1995 was not exceptional. It must be noted that the reconstructions are annual proxies and may not show changes in winter or spring precipitation. It should also be noted that extended wet periods appear to occur more frequently the 20th century (Figure 4a, b). Thus, although the climate of the 20th century does seem to have slightly more variable streamflow and indications of extended wet periods, it is difficult to state clearly that recent periods are unusual versus the previous three centuries. We therefore conclude that, as of 1995, annual precipitation and streamflow over the previous 50 years appear to have been within the range of natural variation since 1651.

We compared our reconstructions with a record of drought for eastern Mongolia, derived from historical documents, extending from 1740-1939 (Mijiddorj and Namhay 1993). There is good agreement with our reconstructions and the historical reconstruction. The best agreements are found after 1880 and with the 1925 drought, which covered an estimated 70% of eastern Mongolia. Between 1880 and 1939 we can only speculate that the historical record may have improved because of increased observations, better spatial coverage or better document preservation. Our reconstructions also give perspective for the historical drought reconstruction for eastern Mongolia (Mijiddorj and Namhay 1993). The tree-ring records show that the 1925 drought was one of the most severe in the last 350 years. Many droughts estimated to cover 50% of eastern Mongolia occurred in 1800s (Mijiddorj and Namhay 1993). Our reconstructions capture these droughts but show more severe droughts in the 1720s and 1730s (Table 2, Figure 4a, b). Also, Mijiddorj and Namhay (1993) stated that a drought in 1827 covered an estimated 70% of their study area. This was neither supported by the reconstructions nor by the raw tree-ring measurements. Interestingly, 1828 has one of the most consistent false rings in the Urgun Nars trees, occurring in 32% of the samples. Previous work has shown false latewood formation in drought sensitive trees to be a result of a seasonal drought followed by normal or wet conditions (Douglass 1919; Villalba and Veblen 1996). The historical drought reconstruction does not have seasonal resolution, so we can only speculate

that a seasonal drought before or early in 1828 caused the formation of the false ring.

The period of pronounced low variability from about 1850-1900 (Figures 4a, b), and the indication that this interval coincides with an out of phase relationship between the 18 and 22-year waveforms (Figure 6a, b, c) is a noteworthy feature of both reconstructions (Figure 4a, b). Interestingly, these waveforms are strikingly similar to bidecadal waveforms identified in tree-ring reconstructions of drought area indices for the western USA (Cook et al. 1997). Further, the waveforms identified by Cook et al. (1997) also show a reduction in amplitude during the middle to late 1800s to early 1900s. In both the Mongolian and western USA reconstructions, these bidecadal waveforms account for at least 10% of the overall variance.

The bidecadal mode of variation is most significant in the KRS streamflow series. It has been suggested that the streamflow parameter may be one of the most sensitive for detection of the influence of the solar cycle on climate, based on the principle that streamflow integrates hydrometeorological effects over a large region, and amplifies small fluctuations in rainfall (Hoyt and Schatten 1997). It has been suggested that the existence of a bidecadal mode of variation in the drought-sensitive reconstructions for the western USA is consistent with possible solar influence (Cook et al. 1997), confirming earlier studies (Mitchell et al. 1979; Stockton et al. 1983). The existence of a similar mode of variation, particularly in the KRS series comprised of two chronologies covering a large geographic area, appears to suggest a similar influence in Mongolia. Quasi-solar periodicities have also been noted in Mongolian meteorological data (Mijiddorj and Namhay 1993) and tree-ring records (Lovelius et al. 1992), as well as in a drought reconstruction from the Hengduan Mountains, China (Wu et al. 1988). The broad-band power spectra in the 10-13 and 20-24 year periodicities indicate other potential forcings of precipitation in Mongolia. Recent paleoclimatic studies suggest the Asian Monsoon has changed in intensity throughout the Holocene (An and Thompson 1998; Feng et al. 1999). Indeed, changes in major circulation systems may have decadal or multi-decadal scale influence. Therefore, the development of a network of sites across Mongolia and further tests are needed to refute or support the hypothesis of some solar forcing on precipitation.

There are a few theoretical mechanisms for the influence of solar activity on precipitation. One is that at the sunspot maximum more energy is put into the Earth's atmosphere. This causes the Hadley cell to expand intensifying the intratropical conversion zone and increasing precipitation while lowering mean surface pressure (Hoyt and Schatten 1997). Modeling efforts using GCMs similarly suggest that variations in solar energy input would alter

tropospheric stability and processes including low pressure systems in the extratropics (National Resource Council 1994). This hypothesized mechanism has been developed further in a recent climate modeling experiment (Shindell et al. 1999). Solar cycle variability was observed in the model to have an effect on the stratospheric ozone layer. Changes in stratospheric ozone and winds affect the flow of energy at altitudes just below these changes, which then affect the next lower levels. This downward control in the atmosphere can cause changes in planetary waves and influence lower atmospheric temperature and pressure. These findings also imply that the observed 10-12 year oscillations in geopotential height near the Earth's surface may be partially driven by solar variability (Shindell et al. 1999). Finally, new research suggests that solar wind may cause the formation of clouds at high latitude (Feynman and Ruzmaikin 1999). The effect on precipitation may be small, making the solar fingerprint hard to detect. Since streamflow data may contain less noise relative to other hydrometeorological variables, its use might improve detection of possible solar effects (Hoyt and Schatten 1997).

5. Summary

High quality tree-ring chronologies were used to reconstruct annual precipitation and streamflow for the data-sparse region of northeastern Mongolia from AD 1651-1995. The tree-ring streamflow model accounted for more variance than the instrumental precipitation data. The hydrometeorological variations observed for the recent period of instrumental data are within the range reconstructed for the past 345 years. The reconstructions herein appear to show more frequent extended wet periods in recent decades. However, this study does not demonstrate unequivocal evidence of an increase in precipitation as suggested by some climate models (e.g. Kattenburg et al. 1996). An overall appraisal of trends in Mongolian precipitation must await a more geographically comprehensive analysis.

The identification of significant periodicities at around 12 and 20-24 years suggests that there is possible evidence for solar influences in these reconstructions for northeastern Mongolia. A period of pronounced low variability around 1850-1900 in both series appears to coincide with an out of phase relationship between two bidecadal modes of variation, a pattern which also appears evident in drought reconstructions in the western USA. These findings lend support to the hypothesis of possible solar influence as reflected in tree-ring time series, first proposed by Douglass (1919). Although we do not have a mechanism for such influence at this time, this convergence of spectral results in these distant continental climates may inspire more attention to the development of hypotheses (Hoyt and Schatten 1997). Development of

additional chronologies from drought-sensitive sites will likely improve the quality of such reconstructions in future efforts while providing more data and coverage with which to test hypotheses on possible influence of solar effects and other forcings on the climate of Mongolia.

Acknowledgments

References

An, Z. S., and L. G. Thompson, 1998: Paleoclimatic change of monsoonal China linked to global change. *Asian Change in the Context of Global Climate Change*, J. Galloway, J. Melillo, Eds., Cambridge University Press, 18-41.

Blasing, T. J., D. N. Duvick, and D. C. West, 1981: Calibration and verification using regionally averaged single station precipitation data. *Tree-Ring Bull.*, **41**, 37-44.

Boninsegna, J. A., 1992: South American dendroclimatological records. *Climate Since A.D. 1500*, R. S. Bradley, P. D. Jones, Eds., Routledge, 446-462.

Briffa, K. R., 1995: Interpreting high-resolution proxy climate data - the example of dendroclimatology. *Analysis of climate data variability, applications of statistical techniques*, H. von Storch, A. Navarra, Eds., Springer, 77-94.

Cleaveland, M. K. and D. W. Stahle, 1989: Tree Ring Analysis of surplus and deficit runoff in the White River, Arkansas. *Water Res. Res.*, **25**, 1391-1401.

Cook, E. R., 1985: A Time Series Analysis Approach to Tree-Ring Standardization. Ph.D. Thesis, University of Arizona, 171 pp.

_____, and G. C. Jacoby, 1983: Potomac River streamflow since 1730 as reconstructed by tree rings. *J. Climate Appl. Meteor.*, **22**, 1659-1672.

_____, and L. A. Kairiukstis (Eds.), 1990: *Methods of Dendrochronology*. Kluwer Academic, 394 pp.

_____, K. R. Briffa, and P. D. Jones, 1994: Spatial regression methods in dendroclimatology: A review and comparison of two techniques. *Int. J. Climatol.*, **14**, 379-402.

_____, D. M. Meko, and C. W. Stockton, 1997: A new assessment of possible solar and lunar forcing of the bidecadal drought rhythm in the western United States. *J. Climate*, **10**, 1343-1356.

D'Arrigo, R. D. and G. C. Jacoby, 1991: A 1000-year record of winter precipitation from northwestern New Mexico, USA: a reconstruction from tree-rings and its relation to El Niño and the Southern Oscillation. *The Holocene*, **1**, 95-101.

Dagvadorj, D. and R. Mijiddorj, 1996: Climate change issues in Mongolia. *Hydrometeorological Issues in Mongolia: Papers in Hydrometeorology*, D. Dagvadorj and L. Natsagdorj, Eds., Mongolia, 79-88.

Dai, A. and K. E. Trenberth, 1998: Global variations in droughts and wet spells: 1900-1995. *Geophys. Res. Lett.*, **25**, 3367-3370.

Douglass, A. E., 1919: *Climatic Cycles and Tree-Growth: A study of the annual rings of trees in relation to climate and solar activity.* Carnegie Institution of Washington, 127 pp.

Draper, N. R. and H. Smith, 1981: *Applied Regression Analysis.* John Wiley & Sons, 709 pp.

Feng, X, H. Cui, K. Tang, and L. E. Conkey, 1999: Tree-ring D as an indicator of Asian Monsoon intensity. *Quat. Res.*, **51**, 262-266.

Feynman, J. and A. Ruzmaikin, 1999: Modulation of cosmic ray precipitation related to climate. *Geophys. Res. Lett.*, **26**, 2057-2060.

Fritts, H. C., 1976: *Tree Rings and Climate.* Academic Press, 567 pp.

Grissino-Mayer, H. D., 1996: A 2129-year reconstruction of precipitation for northwestern New Mexico, USA. *Tree Rings, Environment and Humanity*, J. S. Dean, D. M. Meko, and T. W. Swetnam, Eds., The University of Arizona, 191-204.

Hale, G. E., 1924: The law of sun-spot polarity. *Natl. Acad. Sci. (USA) Proc.*, **10**, 53-55.

Holmes, R. L. 1983. Computer-assisted quality control in tree-ring data and measurement. *Tree-Ring Bull.*, **43**, 69-78.

Hoyt, D. V. and K. H. Schatten, 1997: Rainfall. *The Role of the Sun in Climate Change.* D. V. Hoyt, and K. H. Schatten, Oxford University Press, 125-142.

Hughes, M. K., X. Wu, X. Shoa, and G. M. Garfin, 1994: A preliminary reconstruction of rainfall in north-central China since A.D. 1600 from tree-ring density and width. *Quat. Res.*, 42, 88-99.

Jacoby, G. J., R. D. D'Arrigo, Ts. Davaajamts, 1996: Mongolian tree rings and 20th-century warming. *Science*, **273**, 771-773.

Jenkins, G. M. and D. G. Watts, 1968: *Spectral analysis and its application*. Holden-Day, pp. 525.

Kattenberg, A., F. Giorgi, H. Grassl, G. A. Meehl, J. F. B. Mitchell, R. J. Stouffer, T. Tokioka, A. J. Weaver, T. M. L. Wigley, 1996: Climate models - projections of future climate. *Climate Change 1995: the Science of Climate Change*, J. T. Houghton, L. G. Meira, B. A. Callander, N. Harris, A. Kattenberg and K. Maskell, Eds., Cambridge University Press, 285-358.

Kramer, P. J. and T. T. Kozlowski, 1979: *Physiology of Woody Plants*. Academic Press, 657 pp.

Linsley R. K., M. A. Kohler and J. L. H. Paulhus, 1949: *Applied Hydrology*, McGraw-Hill, 689 pp.

Lovelius, N. V., Ts. Davaajamts, and P. D. Gunin, 1992: Dendroindications of forest growth conditions in Mongolia and possibilities of forecasting (in Russian). *Ecology and Use in Nature of Mongolia*, Russian Academy of Sciences, 32-49.

Mann, M. E. and J. M. Lees, 1996: Robust estimation of background noise and signal detection in climatic time series. *Climatic Change*, **33**, 409-445.

Marple, S. L., Jr., 1987: *Digital Spectral Analysis with Applications*. Prentice-Hall, 289 pp.

Meiyu, Y., L. Yimin, and D. Min, 1995: The influence of sea surface temperature anomaly on seasonal precipitation and temperature in northwest China and central Asia. *Climatic Change in Arid and Semi-Arid Region of the Central Asia*, Mongolia Hydrometeorological Service, 13-20.

Mijiddorj, R. and A. Namhay, 1993: On Drought and unfavorable winter conditions recurrence in Mongolia (in Russian). *Transactions of the HMRI*, **11**, 118-131.

Mitchell, J. M., Jr., C. W. Stockton, and D. M. Meko, 1979: Evidence of a 22-year rhythm of drought in the western United States related to the Hale solar cycle

since the 17th century. *Solar-Terrestrial Influences on Weather and Climate*, B. M. McCormac and T. A. Seliga, Eds., D. Reidal, 125-144.

National Resource Council, 1994, Solar variations and climate change. *Solar influences on Global Change*, E. A. Frieman Ed., National Academy Press, 23-47.

Percival, D. B., and A. T. Walden, 1993: Multitaper spectral estimation. *Spectral Analysis for Physical Applications: Multitaper and Conventional Univariate Techniques*, Percival, D. B., and A. T. Walden, Cambridge University Press, 331-377.

Price, M. P. and N. D. Simpson, 1913: An account of the plants collected by Mr. M. P. Price on the Carruthers-Miller-Price expedition throughout northwest Mongolia and Chinese Dsungaria in 1910. *J. Linn. Soc. Bot.*, **41**, 385-456.

Samel A. N., W. C. Wang, and X. Z. Liang, 1999: The monsoon rainband over China and relationships with the Eurasian circulation. *J. Climate*, **12**, 115-131.

Schulman, E., 1945: Tree-rings and runoff in the South Platte River basin. *Tree-Ring Bull.* **11**, 18-24.

Shindell, D., D. Rind, N. Balachandran, J. Lean, and P. Lonergan 1999: Solar cycle variability, ozone, and climate. *Science,* **284**, 305-308.

Shove, D. J., 1983: Editor's comments on papers 24 through 28. *Sunspot Cycles*, D. J. Shove, ed., Hutchinson Ross Publishing Company, 192-198.

Stahle, D. W. and M. K. Cleaveland, 1992: Reconstruction and analysis of spring rainfall over the southeastern U.S. for the past 1000 years. *Bull. Am. Met. Soc.*, **73**, 1947-1961.

Stockton, C. W. and G. C. Jacoby, 1976: Long-term surface-water supply and streamflow trends in the Upper Colorado River basin based on tree-ring analyses. *Lake Powell Research Project Bull.*, **18**, 70 pp.

Stockton, C. W., J. M. Mitchell, and D. M. Meko, 1983: A reappraisal of the 22-year drought cycle. *Solar-Terrestrial Influences on Weather and Climate*, B.M. McCormac, Ed., Colorado Associated University Press, 507-515.

Stokes M. A. and T. L. Smiley, 1968. *An Introduction to Tree-Ring Dating*. University of Chicago Press, 73 pp.

Vautard, R., 1995: Patterns in time: SSA and MSSA. *Analysis of climate variability, applications of statistical techniques*, H. von Storch and A. Navarra, Eds., Springer, 259-279.

Villalba, R. and T. T. Veblen. 1996. A tree-ring record of dry spring-wet summer events in the forest-steppe ecotone, northern Patagonia, Argentina. *Tree Rings, Environment and Humanity*, J. S. Dean, D. M. Meko, and T. W. Swetnam, Eds., The University of Arizona, 107-116.

Wang, C. W., 1961: *The Forests of China*. Cabot Foundation Pub. No. 5., Harvard University Press, 313 pp.

Wigley, T. M. L., K. R. Briffa, and P. D. Jones, 1984: On the average value of correlated time series, with applications in dendroclimatology and hydrometeorology. *J. Clim. Appl. Meteor.*, **23**, 201-213.

Wu, X. D., 1992: Studies in China. *Climate Since A.D. 1500*, R. S. Bradley, and P. D. Jones, Eds., Routledge, Chapman and Hall, Inc., 437-443.

_____, L. Zhenyao, and S. Li, 1988: A preliminary study on the climatic change of the Hengduan Mountains area since 1600 A.D. *Advanc. Atmos. Science*, **5**, 437-443.

Xue, Y., 1996: The impact of desertification in the Mongolian and the Inner Mongolian grassland on the regional climate. *J. Climate*, **9**, 2173-2189.

Yatagai, A. and T. Yasunari, 1994: Trends and decadal-scale fluctuations of surface air temperature and precipitation over China and Mongolia during the recent 40 year period (1951-1990). *J. Met. Soc. Japan.*, **72**, 937-957.

Yatagai, A. and T. Yasunari, 1995: Interannual variations of summer precipitation in the arid/semi-arid regions in China and Mongolia: their regionality and relation to the Asian Summer Monsoon. *J. Met. Soc. Japan.*, **73**, 909-923.

Young, K. C., 1994: Reconstructing streamflow time series in central Arizona using monthly precipitation and tree ring records. *J. Climate*, **7**, 361-374.

Zhang, J. and Z. Lin, 1992: *Climate of China*. Wiley, 376 pp.

Figure Captions:

Figure 1. Location of sampling sites and meteorological stations in Mongolia. A tree symbol ( ) represents the Urgun Nars and Zuun Mod sites. Tree site names are bold. Hollow circles (O) are meteorological stations. The solid circle (●) represents the streamflow gage location. The shaded area approximates the watershed modeled. Only the mountain range of the watershed is pictured.

Figure 2. Monthly correlation coefficients of a) Urgun Nars tree-ring chronology and instrumental precipitation data and b) Urgun Nars (stipled bars) and Zuun Mod (solid bars) tree-ring chronologies with instrumental Kherlen River streamflow data.

Figure 3. Recorded (solid line) and reconstructed (dashed line) a) Urgun Nars precipitation from 1942-1995 and b) Kherlen River streamflow from 1948-1994.

Figure 4. Reconstruction of a) Urgun Nars precipitation and b) Kherlen River streamflow. The thin line is reconstructed data. The thick, curvilinear line is the 10 year cubic smoothing spline. The solid, flat line is the reconstruction mean. Filled ovals signify extreme wet intervals. Filled rectangles signify extreme dry intervals. Extreme intervals were averaged over 5 year periods and ranked to identify the top 10 wet and dry five-year intervals.

Figure 5. MTM spectral densities of a) Urgun Nars precipitation reconstruction and b) Kherlen River streamflow reconstruction. The thick solid line = the null hypothesis. Dot and dashed line = the 90% confidence level; Dashed line = 95%; Solid line with diamonds = 99%. Centers of the peaks are labeled in years. The null hypothesis was determined using the robust noise background estimation procedure (Mann and Lees, 1996).

Figure 6. a) 10 year running average of the Kherlen River streamflow reconstruction (KRS). The solid, flat line shows the reconstruction mean. b) 21 year waveform of UNP extracted by SSA. c) The 22 (thick line) and 18 (dashed line) year waveforms extracted from KRS using SSA. The shaded areas show intervals of reduced streamflow (a) and precipitation amplitude (b) that correspond to intervals when the 22 and 18 year waveforms are out of phase (c).

Figure 7. MEM spectrum of the UNP 21 year waveform. Centers of the peaks are labeled in years.